

# Chemical-Empowered Human Adipose-Derived Stem Cells with Lower Immunogenicity and Enhanced Pro-angiogenic Ability Promote Fast Tissue Regeneration

Junzhi Yi,<sup>1,2,3,†</sup> Jiayan Zhang,<sup>1,2,3,†</sup> Qin Zhang,<sup>1,2,3,6,†</sup> Xuri Chen,<sup>1,2,3</sup> Rujie Qi,<sup>1,2,3</sup> Renjie Liang,<sup>1,2,3</sup> Ying Wang,<sup>1,2,3</sup> Fei Wang,<sup>1,2,3</sup> Yuliang Zhong,<sup>1,2,3</sup> Xianzhu Zhang,<sup>1,2,3</sup> Grace Chin,<sup>1,2,3</sup> Qi Liu,<sup>1,2,3</sup> Wenyan Zhou,<sup>1,2,3</sup> Hua Liu,<sup>1,2,3</sup> Jiansong Chen,<sup>5,\*</sup> Hongwei Ouyang,<sup>1,2,3,4,\*</sup>

<sup>1</sup>Dr. Li Dak Sum & Yip Yio Chin Center for Stem Cells and Regenerative Medicine, and Department of Orthopedic Surgery of the Second Affiliated Hospital, Zhejiang University School of Medicine, Hangzhou, People's Republic of China

<sup>2</sup>Department of Sports Medicine, Zhejiang University School of Medicine, Hangzhou, People's Republic of China

<sup>3</sup>Zhejiang University-University of Edinburgh Institute, Zhejiang University School of Medicine, and Key Laboratory of Tissue Engineering and Regenerative Medicine of Zhejiang Province, Zhejiang University School of Medicine, Hangzhou, People's Republic of China

<sup>4</sup>China Orthopedic Regenerative Medicine Group (CORMed), Hangzhou, People's Republic of China

<sup>5</sup>Department of Orthopedic Surgery, The Children's Hospital, Zhejiang University School of Medicine, National Clinical Research Center for Child Health, Hangzhou, People's Republic of China

<sup>6</sup>Institute of Translational Medicine, Shanghai University, Shanghai, People's Republic of China

\*Corresponding authors: Hongwei Ouyang, Dr. Li Dak Sum & Yip Yio Chin Center for Stem Cells and Regenerative Medicine, and Department of Orthopedic Surgery of the Second Affiliated Hospital, Zhejiang University School of Medicine, Hangzhou, People's Republic of China. Email: [hwoy@zju.edu.cn](mailto:hwoy@zju.edu.cn) or Jiansong Chen Department of Orthopedic Surgery, The Children's Hospital, Zhejiang University School of Medicine, National Clinical Research Center for Child Health, Hangzhou, People's Republic of China. Email: [ericchen225@163.com](mailto:ericchen225@163.com)

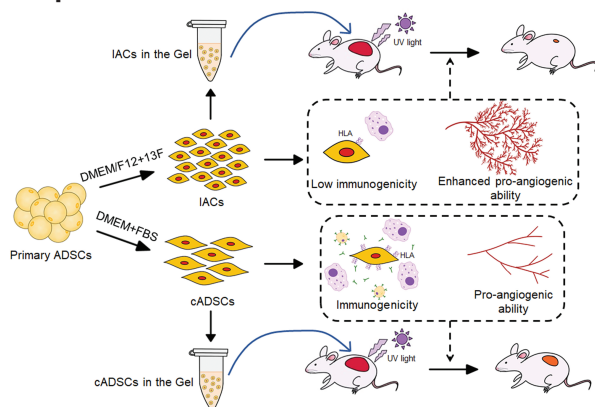
†These authors contributed equally to this work.

## Abstract

Mesenchymal stem cells (MSCs) have been widely used as functional components in tissue engineering. However, the immunogenicity and limited pro-angiogenic efficacy of MSCs greatly limited their pro-regenerative ability in allogeneic treatment. Herein, utilizing a chemically defined cocktail in the culture system, including cytokines, small molecules, structural protein, and other essential components, we generated the immunoprivileged and pro-angiogenic cells (IACs) derived from human adipose tissues. Conventional adipose-derived MSCs (cADSCs) were used as a control in all the experiments. IACs show typical MSC properties with enhanced stemness capacity and a robust safety profile. IACs induce a significantly milder immune response of allogeneic peripheral blood mononuclear cells in an H3K27me3-HLA axis-dependent manner. IACs, through superior paracrine effects, further promote nitric oxide production, anti-apoptotic ability, and the tube formation of human vein endothelial cells. Embedded in a photo-reactive hydrogel (Gel) termed as GelMA/HA-NB/LAP for tissue engineering treatment, IACs promote faster tissue regeneration in a xenogeneic full-thickness skin defect model, eliciting a milder immune response and enhanced blood vessel formation in IACs-treated defect areas. Together with its excellent pro-regenerative potential and robust safety, our findings suggest that IACs may be a promising candidate for clinically relevant stem cell and tissue engineering therapeutics.

**Key words:** mesenchymal stem cells; tissue engineering; immunogenicity; angiogenesis.

## Graphical Abstract



Received: 23 August 2021; Accepted: 4 February 2022.

© The Author(s) 2022. Published by Oxford University Press.

This is an Open Access article distributed under the terms of the Creative Commons Attribution-NonCommercial License (<https://creativecommons.org/licenses/by-nc/4.0/>), which permits non-commercial re-use, distribution, and reproduction in any medium, provided the original work is properly cited. For commercial re-use, please contact [journals.permissions@oup.com](mailto:journals.permissions@oup.com).

## Introduction

Mesenchymal stem cells (MSCs) have the ability to promote tissue repair and/or alleviate tissue impairment by “hit-and-run” survival and regulation.<sup>1,2</sup> Albeit having been clinically tested as treatment modalities for many diseases such as osteoarthritis and graft versus host disease (GVHD),<sup>2</sup> the therapeutic effects of MSCs are still limited and unsatisfactory.

MSCs display an immunomodulatory capacity by suppressing the immune response both *in vitro* and *in vivo*.<sup>3</sup> Nevertheless, allogenic MSCs (allo-MSCs) are also considered immunogens. Allo-MSCs are not as immunogenic as allogenic fibroblasts and hematopoietic stem cells (HSCs),<sup>1,4</sup> but they can stimulate the proliferation and infiltration of immune cells, which will subsequently attack and eliminate the targeted allo-MSCs.<sup>4,6</sup> This would lead to another drawback of using allo-MSCs, which is the establishment of T-cell memory upon initial exposure of allo-MSCs, rendering the repetition of allo-MSCs treatment more challenging.<sup>5,7</sup> Previous studies reported that increasing the number and promoting the retention of MSCs would enhance the regenerative effects.<sup>3,8</sup> Therefore, reducing the immune rejection of MSCs by decreasing their immunogenicity may also be a good way to improve the functionality of MSCs.

On the other hand, within the short survival period of allo-MSCs, they have shown the ability to promote the formation of blood vessels by the paracrine of pro-angiogenic factors.<sup>9,10</sup> For instance, MSCs have been reported to enhance the tube formation of human umbilical vein endothelial cells (HUVECs) *in vitro*; preserve capillary density for alleviating the myocardial infarction-induced impairment; and promote the formation of blood vessels for skin wound repair by secretion of pro-angiogenic factors.<sup>9,10</sup> Since neovascularization is a key step in the process of tissue regeneration, promoting angiogenesis will often accelerate tissue regeneration.<sup>9,11,12</sup> Further enhancing the pro-angiogenic ability of MSCs should be a strategy for fast tissue repair. A previous study reported that enhancing the pro-angiogenic ability of MSCs by adenovirus-mediated *N-Cadherin* gene transduction further promote heart repair.<sup>9</sup> However, the cells modified by virus and treated with undefined factors are difficult for clinical use. Therefore, there still remains an intriguing challenge in the immunogenicity reduction and the pro-angiogenic ability reinforcement of MSCs in a safe way.

Herein, we assumed that utilizing a chemically defined culture system, the factors in which could not only support cell expansion but also empower cells in angiogenic ability and/or immunogenicity would be a secured way to tackle both challenges in cell function and safety. Bone marrow-derived MSCs (BMSCs) and adipose-derived MSCs (ADSCs) are the most frequently used MSCs in clinical trials.<sup>13</sup> Between these 2 MSC populations, ADSCs have been previously revealed to exhibit higher pro-angiogenic capability and lower immunogenicity, respectively.<sup>13,14</sup> Therefore, human adipose tissues were used as a cell source and conventional ADSCs (cADSCs) were used as a control. In this study, we generated the immunoprivileged and pro-angiogenic cells (IACs) by utilizing the chemically defined cocktail as their culture medium. The cultured IACs display a typical MSC phenotype while exhibiting lower immunogenicity and higher pro-angiogenic capacity. Owing to the abovementioned characteristics, the IACs we generated successfully further promoted tissue regeneration in a full-thickness skin wound model when cells are incorporated into a photo-reactive hydrogel

termed as GelMA/HA-NB/LAP (Gel) developed in our previous studies.<sup>11,15</sup>

## Materials and Methods

### Culture System for IACs

Besides using DMEM/F12 (Gibco) as a basal medium, other 13 kinds of chemically defined cocktail factors (13F) included 1× Insulin-Transferrin-Selenium (ITS; Gibco, 41400-045), 0.1% lipid concentrate (Gibco, 11905-031), 2 ng/mL TGF-β1 (Peprotech, AF-100-21C), 5 ng/mL bFGF (Peprotech, 100-18B), 10 ng/mL PDGF-AB (Peprotech, 100-00AB), 10 ng/mL PDGF-BB (Peprotech, 100-14B), 1 μg/mL fibronectin (Novoprotein, CH38), 197.6 μM vitamin C (Sigma, A8960), 55.9 μM putrescine (Sigma, P5780), 17.8 nM progesterone (Selleck, S1705), 100 nM hydrocortisone (Selleck, S1696), 10 μg/mL heparin sodium (Selleck, S1346), and 1.722 g/L sodium bicarbonate (NaHCO<sub>3</sub>, Gibco, 25080-094).

### Cell Passage and the Inhibition of H3K27me3

cADSCs were cultured with “L-DMEM + 10% FBS + 1% P/S” while IACs were cultured with “DMEM/F12 + 13F”. When the cells reached 80-90% confluence, they were digested in preheated TrypLE (Gibco) at 37 °C. After centrifugation, the cells were resuspended and seeded at different densities according to different experimental needs. In this study, cells at P3 and P5 (cells that have been digested 3 and 5 times, respectively) were used for experiments. For the inhibition of H3K27me3, 10 μM EPZ-011989 (Selleck) was added into the culture medium 96 hours before experimental tests.

### Co-culture with PBMCs

Peripheral blood mononuclear cells (PBMCs) were isolated from peripheral blood of healthy donors using Ficoll-Paque PLUS (GE Healthcare) according to our previous protocol.<sup>4</sup> To verify the immunosuppressive functions of cADSCs and IACs, isolated PBMCs were stained with CFDA-SE (Beyotime). Next, the PBMCs were stimulated by 100 ng/mL lipopolysaccharide (LPS; Sigma) and then co-cultured with cADSCs or IACs in a 24-well plate. The proliferation of PBMCs was analyzed by FACS at day 3. To test the simulative effects of cADSCs and IACs to PBMCs, the PBMCs were not stimulated by LPS and were co-cultured with the MSCs for 12 days. The supernatants were used for ELISA testing while the cADSCs and IACs were used for viability assay by CCK8. The PBMC culture medium composed of RPMI 1640 (Gibco), 10% FCS, 1% P/S, 50 μM 2-mercaptoethanol (Millipore), 1 mM sodium pyruvate (Gibco) and 1 × L-glutamine (Gibco). To produce FCS, FBS was heated to 56 °C for 30 minutes to inactivate the complements.

### Tube Formation Assay

The conditioned media (CM) of cADSCs (cADSCs-CM) and IACs (IACs-CM) were produced by culturing corresponding cells with L-DMEM for 24 h. HUVECs cultured with cADSCs-CM and IACs-CM were used in different experiments. For the tube formation assay, 100 μL Matrigel (BD Biosciences) was added to each well of a 48-well plate and then polymerized at 37 °C for an hour before experiments. The HUVECs were resuspended and seeded onto the preheated Matrigel at a density of 60 000/cm<sup>2</sup> and incubated for 4-6 h. Tube formation was observed under an inverted microscope and quantified by ImageJ.



## HUVEC Activation and Detection of NO Production

The activation of HUVECs was performed by referencing a previous study with slight modifications.<sup>8</sup> Briefly, HUVECs were treated with L-DMEM containing 100 ng/mL TNF- $\alpha$  for 24 h. Next, the activated HUVECs (aHUVECs) were treated with corresponding CM for another 24 h and then were used for the assay. For the detection of NO production, 3-amino,4-aminomethyl-2',7'-difluorescein diacetate (DAF-FM, Beyotime) test was performed according to the manufacturer's instruction.

## Synthesis of the Gel

GelMA/HA-NB/LAP (Gel), composed of gelatin methacrylate (GelMA), N-(2-aminoethyl)-4-(4-(hydroxymethyl)-2-methoxy-5-nitrosophenoxy) butanamide (NB) linked hyaluronic acid (HA-NB) and trimethylbenzoylphosphinate (LAP), was synthesized and stored as we described previously.<sup>11,15</sup> The final concentration of GelMA, HA-NB and LAP are 5%, 1.25%, and 0.1% (m/v), respectively. For in vitro cytocompatibility assay and in vivo test in the animal model, the cells were harvested, centrifuged, and resuspended in the Gel solution at the concentration of  $2 \times 10^6$ /mL and  $1 \times 10^7$  mL<sup>-1</sup>, respectively.

## Full-Thickness Skin Wound Model

All animals were treated according to the guidelines approved by the Zhejiang University Ethics Committee (ZJU20210054). Eight-week-old SD male rats were used in this study. A full-thickness skin wound model was established as previously described.<sup>11</sup> Briefly, 32 rats were randomized and divided into 4 groups: spontaneous repair (control), the addition of GelMa/HA-NB/LAP (Gel), the addition of the Gel and cADSCs at P3 (Gel + cADSCs), and adding the Gel and IACs

at P3 (Gel + IACs). Circular skin defects with 10 mm in diameter were generated on the back of the anesthetized rats, using a perforated biopsy instrument with a moderate force. Then, the Gel solution or the mixture of the Gel and the cells was dripped and filled into the corresponding defects. After illumination with 365 nm UV light for 6-8 s, the gel solution transformed from viscous liquid to tissue-adhesive hydrogel.<sup>11</sup> After the surgery, all the wounds were covered by commercially available transparent film dressing (Tegaderm Film, 3 M, MN). To quantitatively evaluate the wound healing efficacy, the rats were placed alongside the metric scale, and their wounds or scars were being photographed on day 0, day 7, and day 21. The wound area was analyzed using ImageJ software.

## Statistical Analysis

All data are expressed as mean  $\pm$  SEM. Statistical analysis was performed using GraphPad Prism 8.0 statistical software. Statistical comparisons were calculated using *t*-test (2 groups) or ANOVA (multiple groups). A *P*-value of  $<.05$  was considered statistically significant.

## Results

### Generation of IACs

In this study, we aimed to generate MSCs with lower immunogenicity and enhanced angiogenesis, and several factors that could empower these functions were selected as candidates (Supplementary Table S1). To fulfill safety requirements, we could only utilize chemically defined factors to achieve cell expansion. First, 2 basal media were compared by assessing cell viability on day 1 and day 5 (Fig. 1A). Compared to cells grown in L-DMEM, those in

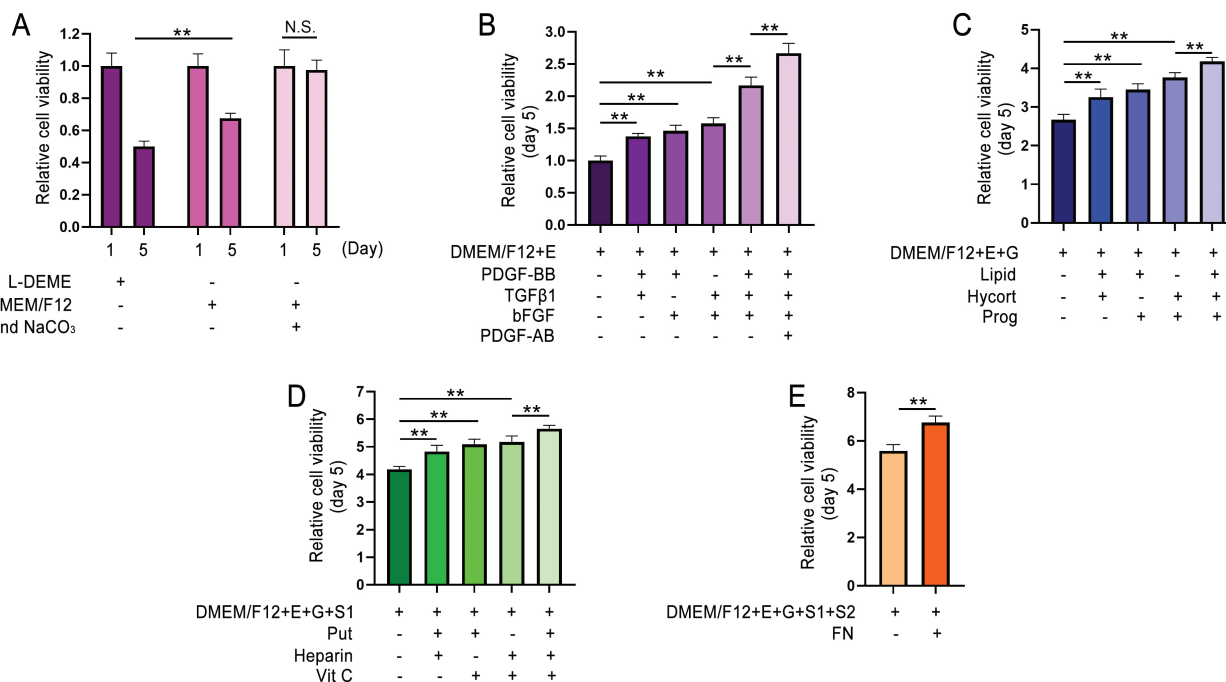


**Figure 1.** Screening of culture factors. (A) Screening of essential components ( $n = 4$ ). (B) Screening of growth factors. "E" represents essential components including Insulin-Transferrin-Selenium (ITS) and NaCO<sub>3</sub> ( $n = 4$ ). (C and D) Screening of small molecules. "G" represents growth factors including bFGF, TGF- $\beta$ 1, PDGF-AB, and PDGF-BB. S1 represents part of small molecules including lipid concentrate (lipid), hydrocortisone (hycort), and progesterone (prog) ( $n = 4$ ). (E) Screening of adhesive factors. S2 represents other parts of small molecules including putrescine (put), vitamin C (Vit C), and heparin sodium (heparin). FN represents fibronectin ( $n = 4$ ). \*\* $P < .01$ .

DMEM/F12 showed relatively higher viability on day 5. After adding ITS and NaHCO<sub>3</sub> into DEME/F12, cell viability kept stable during the 5-day culture. Based on the basal medium with the essential components (ITS and NaHCO<sub>3</sub>), growth factors were screened by assessing cell viability at day 5. The combination of PDGF-BB, TGF-β1, bFGF, and PDGF-AB showed the best effect (Fig. 1B). Then, small molecules were screened. A combination of lipid concentrate (lipid), hydrocortisone (hycort), progesterone (prog), putrescine (put), heparin sodium (heparin), and vitamin C (Vit C) were verified most efficient to promote cell proliferation (Fig. 1C, 1D). Finally, fibronectin (FN) was coated to further improve cell viability (Fig. 1E). The detailed information for all the factors was provided in the method part and Supplementary Table S1.

IACs were derived from primary human ADSCs by culturing the cells with DMEM/F12 supplied with these 13 factors (13F), while cADSCs were cultured with the conventional medium. At least 3 IACs lines were generated for in vitro experiments. The population doubling time (PDT) of IACs and cADSCs was comparable from P1 to P5 (Fig. 2B); the positive rate of Ki67 expression also demonstrated no significant difference at both P3 and P5 (Supplementary Fig. S1A), indicating that the proliferation rates between the 2 groups are comparable.

### IACs Display Typical MSC Properties with Higher Stemness

In most cases, the MSCs used in regenerative medicine are ranged from passage 3 (P3) to passage 5 (P5). Therefore, IACs at P3 and P5 were used for our in vitro experiments (Fig. 2A). IACs manifested a typical spindle-like morphology (Fig. 2E), and a significantly decreased cell area with a relatively higher nuclear-to-cytoplasm ratio compared with those of cADSCs (Fig. 2E and Supplementary Fig. S1B).

Next, we analyzed the typical MSC properties of IACs, which include the ubiquitous surface markers and tri-lineage differentiation capacity. Similar to cADSCs, more than 95% of IACs were stained positive for CD90, CD73, and CD105, and less than 2% IACs were stained positive for CD34, CD45, CD31, and CD144 (Fig 2C and D and Supplementary Fig. S2). After osteoinduction, the calcium deposition and the expressions of osteogenic markers, *Runx2* and *ALP*, were significantly higher in the IAC group compared with the cADSC group at both passaging stages (Fig. 2F, Supplementary Fig. S3A and B). Despite having larger and thicker chondrogenic pellets in the IAC group, both the glycosaminoglycan (GAG)-to-DNA ratios and the expression levels of chondrogenic markers (*Sox9* and *ACAN*) failed to reveal significant differences between the IAC group and cADSC group at both P3 and P5 (Fig. 2G, Supplementary Fig. S3C and D). As for adipogenesis, we found that there were a significantly higher amount of lipid formation and higher expression levels of adipogenic markers (*PPARγ* and *LPL*) in IACs than those of cADSCs at P3, while showing no significant difference at P5 (Fig. 2H, Supplementary S3E and F). Besides, compared with cADSCs, IACs displayed enhanced colony formation ability and elevated C-myc expression at both mRNA and protein levels at P3 and P5 (Fig. 2I and J and Supplementary Fig. S4).

In general, IACs display typical MSC properties and display enhanced stemness capacity compared with cADSCs.

### RNA-seq Analysis of cADSCs and IACs

To find the difference of gene expression profile between IACs and cADSCs, RNA-seq was performed in the 2 groups. KEGG analysis revealed the upregulation of Akt pathway, FAK pathway and PPAR pathway in IACs at both P3 and P5 in addition to the upregulated cell metabolism (Fig. 3A and B). The upregulation of these 3 pathways is related to the enhancement of stemness capacity and pro-angiogenic capability.<sup>16-20</sup> Western blot (WB) analysis proved the results. Relative expressions of key proteins in the Akt pathway, p-Akt, p-PI3K, and p-mTOR, were higher in IACs than those of cADSCs (Fig. 3C). Likewise, the relative levels of key proteins in the FAK pathway, which includes ITGβ1, p-Src, and p-FAK, were also higher in IACs (Fig. 3D). In the PPAR pathway, relative expression levels of FABP1 and PPARδ were also significantly higher in IACs while PPARγ was lower in IACs (Fig. 3E). In contrast with FABP1 and PPARδ, PPARγ plays an important role in adipogenic differentiation,<sup>21</sup> a lower level of PPARγ hence translate into higher stemness. Besides, it is worth noting that previous studies have widely linked higher stemness with lower immunogenicity.<sup>4,22-27</sup> Although the immunogenicity-related terms were not ranked in the top 10 in KEGG analysis, key genes that determine the immunogenicity, including those that encode for MHC class I complexes (*B2M* and *HLA-C*) and IFN-γ response factors (*IRF1* and *IRF6*),<sup>27</sup> were downregulated in IACs as observed in the RNA-seq data (Fig. 3F). Taken together, these results reinforce the possibility that IACs display higher stemness, lower immunogenicity and enhanced pro-angiogenic ability compared to cADSCs (Fig. 3G).

### IACs Display Lower Immunogenicity

Given the low expressions of key genes that are related to immunogenicity in RNA-seq data and because IACs display higher stemness, we then investigated the immunogenicity of IACs. HLA-ABC plays a key role in triggering immune response while HLA-G functions in immune tolerance.<sup>4,5,28</sup> Our immunofluorescence (IF) assays showed that the expression of HLA-ABC was significantly lower while the expression of HLA-G was higher in IACs compared with cADSCs (Fig. 4A and B). Similarly, the relative mRNA levels of *HLA-A*, *HLA-B*, *HLA-C*, and *B2M* loci were lower in the IAC group while the mRNA levels of *HLA-G* were higher in the IAC group compared with those of cADSCs (Fig. 4C and D). Albeit showing comparable abilities to inhibit the proliferation of LPS-stimulated allogenic PBMCs (Supplementary Fig. S5), both IACs and cADSCs can serve as immunogen as they would stimulate a higher secretion of inflammatory factors of unstimulated PBMCs as relative to the PBMC alone group (Fig. 4F). After the cells were co-cultured with unstimulated allogenic PBMCs (Fig. 4E), the TNF-α and IFN-γ contents were higher in the co-culture system containing PBMCs and cADSCs than those in the system containing PBMCs and IACs (Fig. 4F). As allogenic PBMCs would kill the co-cultured MSCs,<sup>5</sup> the cell viabilities of IACs and cADSCs were also measured after the co-culture. IAC group showed significantly higher cell viability than those of the cADSC group 12 days after the co-culture (Fig. 4G), indicating that the PBMC-mediated cytotoxicity for IACs is milder.

We next further investigated the underlying mechanism of how IACs display lower immunogenicity. A previous

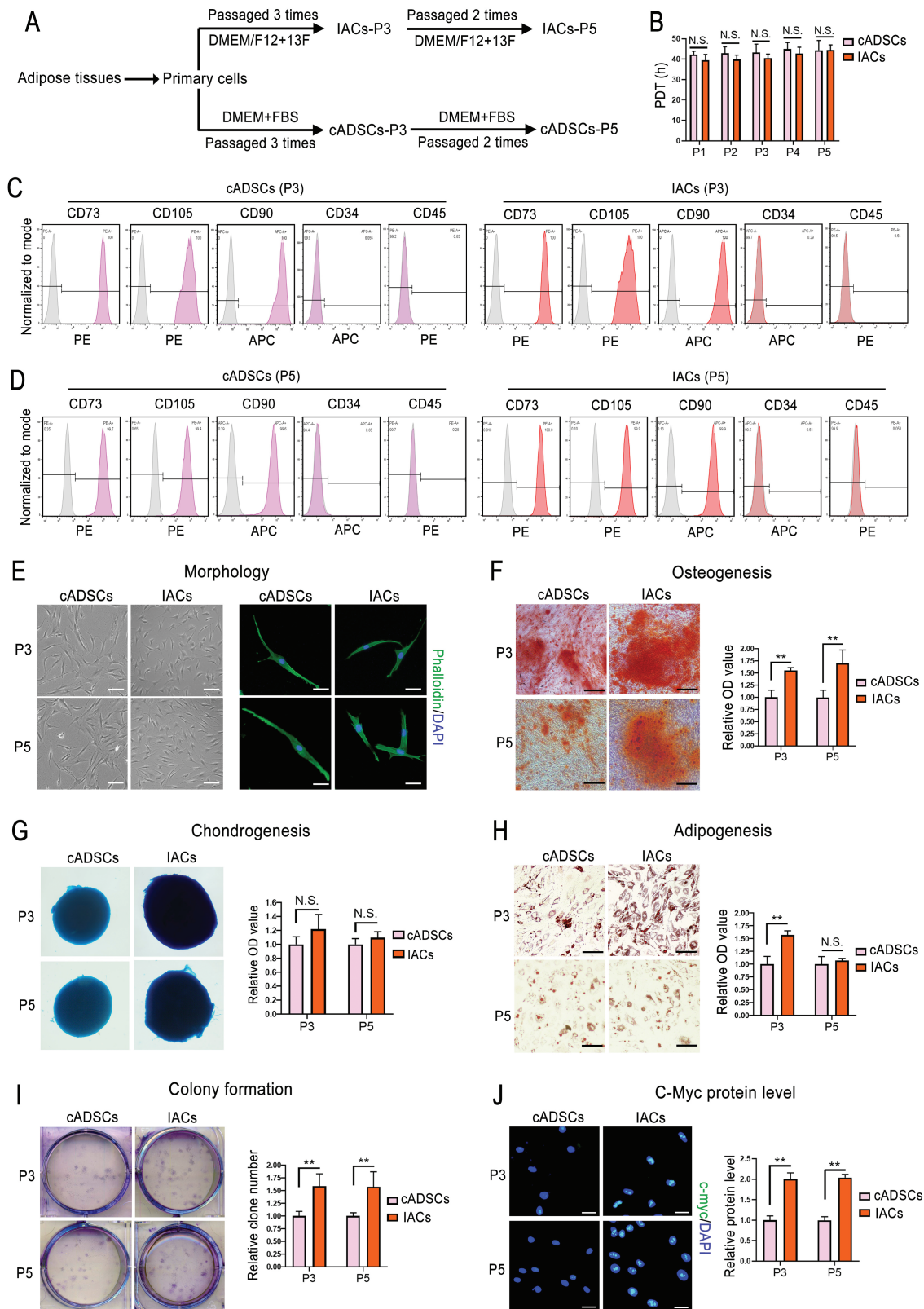


**Figure 2.** The typical properties of IACs. **(A)** Schematic illustration of the generation of IACs. **(B)** Population doubling time (PDT) for IACs and cADSCs ( $n = 3$ ). **(C)** and **(D)** Surface marker analysis of IAC and cADSC by flow cytometry. The gray peaks indicate the isotype control. **(E)** Representative morphology of cADSCs and IACs in the light field (right panel) and IF staining of Phalloidin and DAPI (left panel). Scale bar = 120  $\mu\text{m}$  (left panel), scale bar = 50  $\mu\text{m}$  (right panel). **(F–H)** Alizarin red (F), Alcian blue (G), and oil red (H) staining of osteogenic cells, chondrogenic pellets, and adipogenic cells. Quantification is respectively showed at corresponding right panel ( $n = 4$ ), scale bar = 150  $\mu\text{m}$  in F and H. **(I)** Colony formation assay of cADSCs and IACs in 6-well plate. A relative number of clones is counted at the right panel ( $n = 4$ ). **(J)** Representative images of IF staining and corresponding quantification of C-Myc protein level for cADSCs and IACs ( $n = 4$ ). Scale bar = 30  $\mu\text{m}$ . \* $P < .05$ , \*\* $P < .01$ .



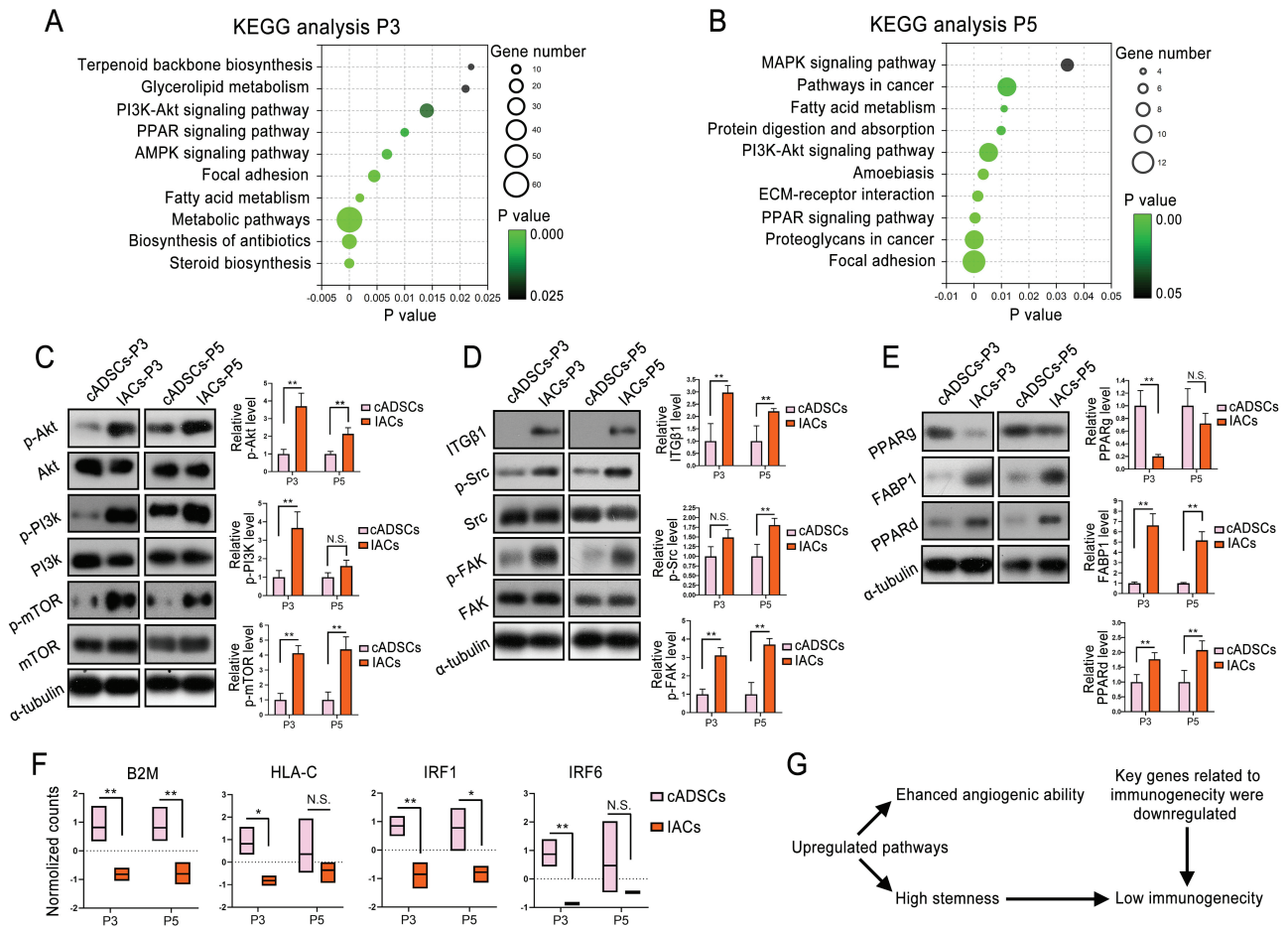


**Figure 3.** RNA-seq analysis of cADSCs and IACs. (A and B) KEGG analysis of the upregulated pathways of IACs at P3 (A) and P5 (B). (C–E) WB validation for the upregulation of PI3K-Akt pathway (C), FAK pathway (D), and PPAR pathway (E) by testing the key proteins in these pathways. Quantification is shown at the corresponding right panel ( $n = 4$ ). (F) The expression levels of key genes that related to immunogenicity from RNA-seq data ( $n = 3$ ). (G) The logic flow of our inference about the advantages of IACs according to RNA-seq data. \* $P < .05$ , \*\* $P < .01$ .

study has reported that a high level of H3K27me3 would keep the HLA-ABC expression level low.<sup>27</sup> Several studies also underline the fact that the elevated H3K27me3 expression level is contingent on the upregulation of both the Akt pathway and the FAK pathway.<sup>29,30</sup> In our study, we used an H3K27me3 inhibitor (H3K27me3i) to downregulate the H3K27me3 protein levels (Fig. 4H). As a result, the HLA-ABC expression levels in IACs + H3K27me3i group were significantly higher than those of the IAC group (Fig. 4I and J). Consequently, when IACs were co-cultured with PBMCs, the inhibition of H3K27me3 reversed the lower secretion levels of inflammatory factors in the IAC group and reversed the PBMC-mediated milder cytotoxicity towards IACs (Fig. 4K).

Therefore, IACs display lower HLA-ABC levels and induce milder inflammatory response and cytotoxicity of PBMCs. These properties of IACs attribute, at least partly, to a higher expression of H3K27me3.

### IACs Display Enhanced Pro-angiogenic Capability

Angiogenesis is an important process during wound healing and both our RNA-seq and WB analysis have shown that IACs displayed some upregulated pathways that are related to angiogenesis (Fig. 3). From this perspective, we compared the pro-angiogenic capability of IACs and cADSCs (Fig. 5A). From

RNA-seq data, some pro-angiogenic genes in the IAC group were observed to be upregulated at both P3 and P5 (Fig. 5B). Besides, the IAC group showed significantly higher mRNA and protein expressions of 2 important pro-angiogenic factors, namely HGF and MMP-13<sup>9</sup> (Fig. 5Aa, C, and D). VEGF expression at both levels was comparable (Fig. 5Aa and Supplementary Fig. S6). On the contrary, IACs showed significantly lower expression of PAI1, an anti-angiogenic factor,<sup>31</sup> at both mRNA level and secreted protein level (Fig. 5Aa, 5E). To further confirm the enhanced pro-angiogenic capacity of IACs by their paracrine effects, the conditioned media of IACs (IACs-CM) and cADSCs (cADSCs-CM) were used to culture HUVECs. Tube formation assay showed that IACs-CM significantly promotes the tube formation of HUVECs compared with those of cADSCs-CM (Fig. 5Ab, 5F). *eNOS* gene mediates nitric oxide (NO) production and NO is responsible for pro-angiogenic functions of endothelial cells. Under an inflammatory environment, where the HUVECs were pre-treated with TNF- $\alpha$  (aHUVECs),<sup>8</sup> the IACs-CM contributed to a significant upregulation of the expression of *eNOS* at both protein (Fig. 5Ac, 5G) and mRNA levels (Fig. 5Ac and Supplementary S7A) and NO production in HUVECs (Fig. 5Ac, 5H and Supplementary Fig. S7B) compared with those of cADSCs-CM. On the other hand, the enhanced pro-angiogenic ability of IACs-CM was revealed by the inhibition of aHUVEC apoptosis. The protein levels of cleaved caspase-3 were lower



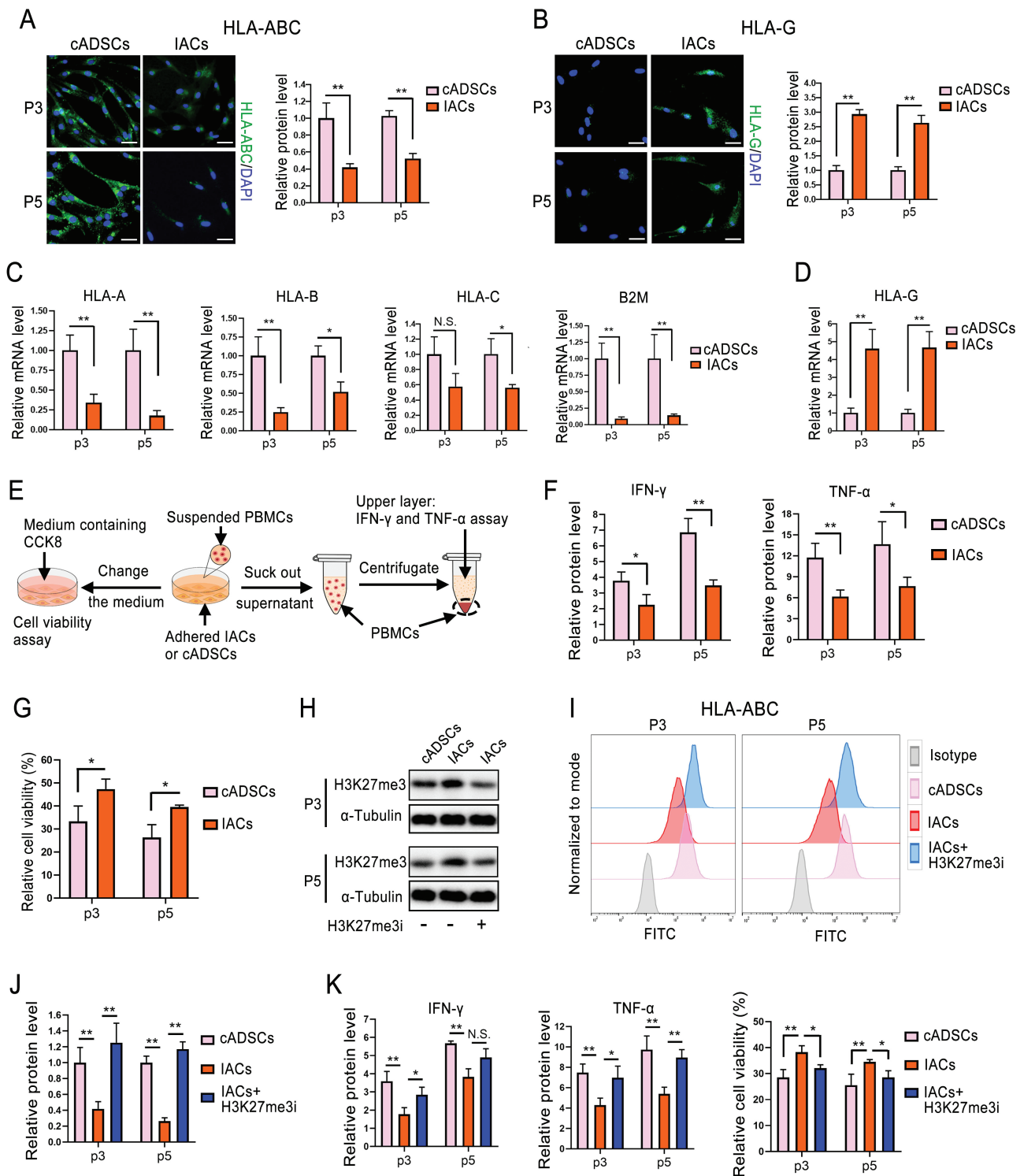


**Figure 4.** The immunoprivilege of IACs compared with cADSCs. (**A** and **B**) Representative images and quantification of IF staining of HLA-ABC (**A**) and HLA-G (**B**) in IACs and cADSCs ( $n = 3$ ). Scale bar = 50  $\mu\text{m}$ . (**C** and **D**) RT-qPCR evaluating the mRNA levels of HLA-A, HLA-B, HLA-C, B2M (**C**), and HLA-G (**D**) in cADSC and IACs ( $n = 3$ ). (**E**) Schematic illustration of the co-culture experiments. (**F**) ELISA assay of secreted IFN- $\gamma$  and TNF- $\alpha$  content in supernatants relative to PBMCs alone group ( $n = 3$ ). (**G**) CCK8 analysis of the cell viability of nADSC and IACs ( $n = 3$ ). (**H**) WB analysis of H3K27me3 protein expression in cADSCs and IACs with or without the inhibitor of H3K27me3 (H3K27me3i). (**I** and **J**) Flow cytometry analysis of HLA-ABC expression in cADSCs and IACs with or without H3K27me3i (**I**) and corresponding quantification (**J**) ( $n = 3$ ). (**K**) Secreted IFN- $\gamma$  and TNF- $\alpha$  content and the cell viability assay after co-culture with PBMCs ( $n = 3$ ). \* $P < .05$ , \*\* $P < .01$ .

in the IACs-CM group; the protein levels of Bcl2 were higher in the same group compared with those of the cADSCs-CM group (Fig. 5Ac, 5I). These results denote the fact that IACs show enhanced pro-angiogenic ability through their paracrine effects.

### The Safety Profile of IACs

It is worth noting that overloaded stemness, immune evasion, and angiogenesis may bring tumorigenic risks. Tumorigenicity assays that we performed revealed that neither IACs nor

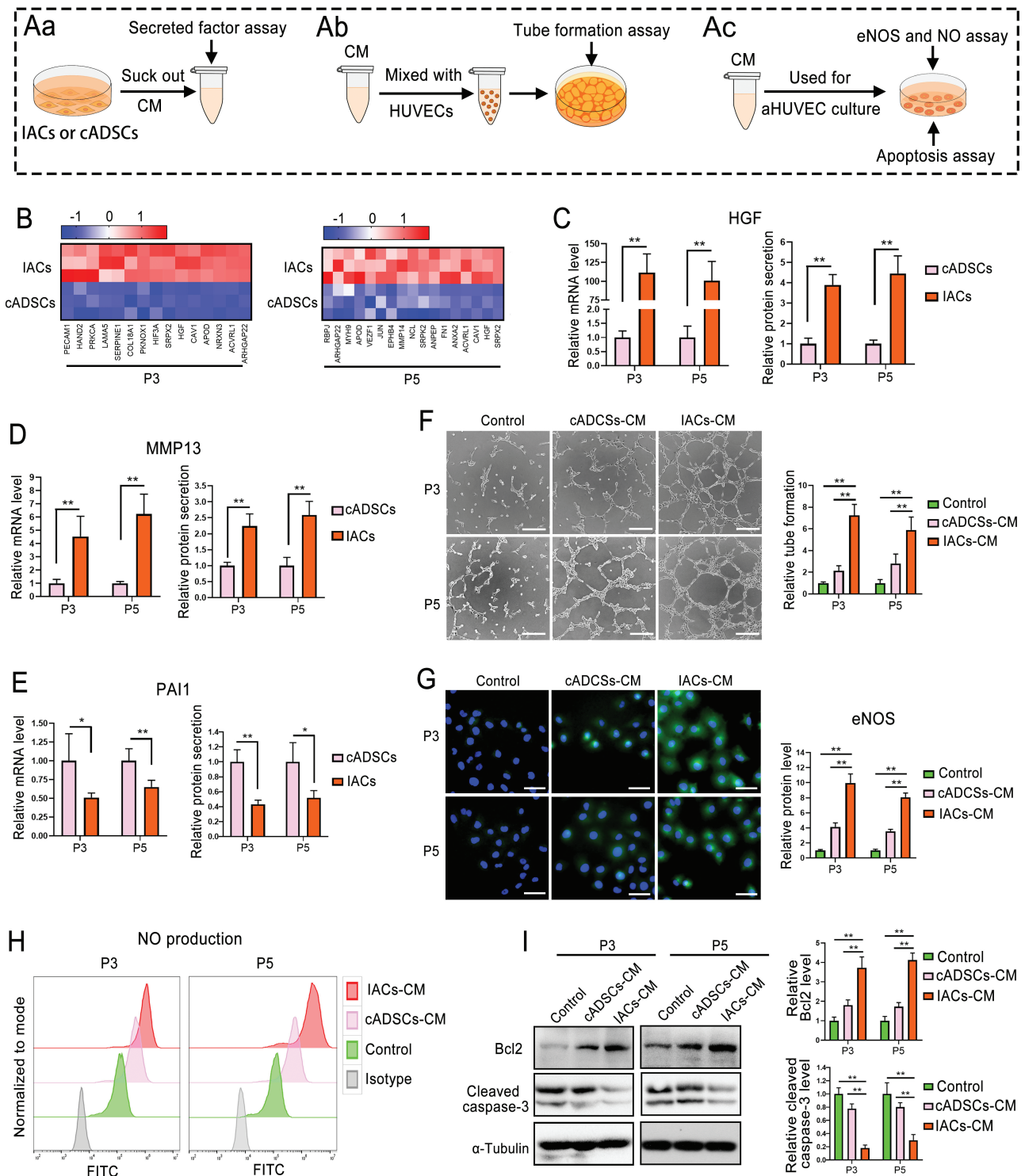


**Figure 5.** The enhanced pro-angiogenic effect of IACs compared with cADSCs. **(A)** Schematic illustration of the analysis of secreted factors (**Aa**), the effect of conditioned media (CM) toward HUVEC tube formation (**Ab**), and the effects of CM toward the eNOS expression, NO production and apoptosis of aHUVECs (**Ac**). **(B)** Heatmap illustrating the upregulated pro-angiogenic genes of IACs. **(C, D, and E)** The expressions of pro-angiogenic cytokines, HGF (**C**) and MMP13 (**D**), and antiangiogenesis-related cytokines PAI1 (**E**) of IACs and cADSCs ( $n = 4$ ). **(F)** Tube formation of HUVECs in control medium, cADSCs-CM, and the IACs-CM. The right panel is the quantification ( $n = 4$ ). Scale bar = 250  $\mu\text{m}$ . **(G)** Representative images of IF staining and the quantification of eNOS protein expression in aHUVECs treated with control medium, cADSCs-CM and IACs-CM ( $n = 3$ ). Scale bar = 50  $\mu\text{m}$ . **(H)** Flow cytometry analysis of NO production in aHUVECs. **(I)** Western blot illustrating the Bcl2 and cleaved caspase-3 expression in aHUVECs. The quantification is presented at the right panel ( $n = 4$ ). \* $P < .05$ , \*\* $P < .01$ .

cADSCs led to tumorigenicity in nude mice for 28 days, nor did they form tumor-like clones in soft agar for 16 days (**Supplementary Fig. S8B and D**). Conversely, HepG2 (human

hepatocellular carcinomas cell line), as a positive control, formed tumors in vivo and many tumor-like clones in vitro (**Supplementary Fig. S8B and D**). Karyotyping analysis showed

that there were no chromosome abnormalities in IACs at both P3 and P5 (Supplementary Fig. S8A). Among the differential gene expression profile in IACs, although the upregulated C-Myc level could be a potential threat that renders IACs oncogenic, the mRNA levels of C-Myc in IACs was still less than  $1/2^5$  of that in embryonic stem cells (ESCs) (Supplementary Fig. S8C). On top of that, the expressions of other pluripotent markers (Oct4, Sox2, and Nanog) were not observed positive in both cADSCs and IACs while ESCs were positive for these expressions (Supplementary Fig. S9). Therefore, we conclude that IACs have a robust safety profile and are eligible for further in vivo experiments.

### IACs Promote Fast Tissue Regeneration in a Full-thickness Skin Defect Model

Given the immunoprivilege and pro-angiogenic ability of IACs, full-thickness skin defects in rats were used as a model to explore the regenerative effects of IACs in vivo. Two IACs lines were used for in vivo study. Our group has previously developed a strongly adhesive hydrogel (Gel) termed GelMA/HA-NB/LAP, which is not only able to fix the living organs through Schiff base reaction upon exposure to UV irradiation but also promote progressive ingrowth of host tissues.<sup>11,15</sup> Therefore, a mixture of the MSCs (P3) and the photo-reactive Gel was used as a tissue-engineering method (Fig. 6A). In vitro 3D cell culture showed that more than 95% of cells were viable at day 1 and day 3 and the cell viability was increased to more than 1.6 folds for both groups of cells for 3 days (Supplementary Fig. S10), indicating that the Gel is cytocompatible enough for loading both groups of cells. After the surgery, the wound areas in the IAC group were the smallest on day 7 and day 21 (Fig. 6B, 6D). HE staining not only illustrated a significantly larger re-epithelialization area and less infiltrated inflammatory cells in Gel + IACs at day 7 (Fig. 6E, 6G) but also showed more appendages in this group at day 21 compared with those of cADSCs + Gel group (Fig. 6F, 6G). As blood vessels and hair follicles are 2 essential appendages in the skin for maintaining its normal functions, the mRNA expressions of markers of the mature blood vessels (CD31 and  $\alpha$ -SMA) and hair follicles (CK15) were measured at day 21 by RT-qPCR. The Gel + IACs group had the highest expression levels of all the markers abovementioned (Supplementary Fig. S11A, S11B, and S11C). These results suggest that IACs show augmented therapeutic effects on cutaneous wound healing compared with that of cADSCs. Besides, both the Gel group and Gel + cADSCs group showed enhanced wound healing compared to the control group.

### IACs Induce a Milder Immune Microenvironment and a Stronger Pro-Angiogenic Microenvironment During Wound Healing

As IACs have shown lower immunogenicity and enhanced pro-angiogenic ability in vitro, we then detected the relative levels of the inflammatory response and angiogenesis in the wound area at day 7 to further clarify the mechanisms of how IACs promote fast tissue regeneration. In consistent with in vitro experiments (co-culture with PBMCs), more immunoprivileged IACs, rather than cADSCs, were retained (Fig. 7B), although both groups of cells were rejected at day 21 (Supplementary Fig. S12). The contents of CD3 and MPO in the wound area were downregulated at both protein and mRNA levels in Gel + IACs group compared with those of the

Gel + cADSCs group (Supplementary Fig. 7C, D, G, H, and K), indicating that Gel + IACs group induces less infiltrated T cells and neutrophils, respectively. The CD206 contents in the wound area were upregulated and the CD11c contents in the wound area were downregulated at both mRNA and protein levels in Gel + IACs group compared with those of the Gel + cADSCs group (Fig. 7E, I, and K), indicating that there are more M2 macrophage (wound healing type) and less M1 macrophage (inflammatory type) in the wound area of Gel + IACs group. Besides, the mRNA levels of inflammatory factors (TNF- $\alpha$  and IL-1 $\beta$ ) were significantly decreased in Gel + IACs group compared with Gel + cADSCs group at this time point (Supplementary Fig. S11D, S11E). On the other hand, the contents of CD133 and CD34 in the wound area of Gel + IACs group were significantly upregulated at both mRNA and protein levels compared with those of Gel + cADSCs (Fig. 7F, 7J, and 7K), indicating that more EPCs exist in the wound area of Gel + IACs group. The expression of VEGF was also significantly upregulated in the wound area of Gel + IACs group compared with Gel + cADSCs group (Supplementary Fig. S11F). In general, IACs induce a milder immune microenvironment and a stronger pro-angiogenic microenvironment in vivo.

## Discussion

To address the pressing need to safely generate MSCs with higher regenerative efficiency, our group sought to utilize a chemically defined cocktail culture system in this study to lower the immunogenicity of the cells while empowering their pro-angiogenic ability. As a consequence, the chemical-empowered IACs showed typical MSC properties with a robust safety profile, enhanced stemness capacity, reduced immunogenicity, and a stronger pro-angiogenic ability. Compared with cADSCs, they further promote tissue regeneration in a xenogenic skin defect model.

First, we reported the generation of IACs by a chemically defined cocktail. For immunogenicity reduction and pro-angiogenic ability reinforcement, the cells were treated with stimulative factors. For achieving the safety requirement, we used only chemically defined factors in cell culture. Therefore, as described in Supplementary Table S1 and Materials and Method, all of the components used in the cell culture could play a role in supporting cell expansion. Most of these components could regulate signaling pathways related to the expression of HLA Class I and/or signaling pathways related to pro-angiogenesis. To the best of our knowledge, this is the first study that achieves targeted empowerment of MSC functions during cell expansion in a safe way. This is similar to our previous study in which chemical-empowered tendon stem cells were generated for tissue repair by utilizing several small molecules.<sup>32</sup> Interestingly, although many upregulated genes in IACs were related to proliferation and stemness, IACs did not display an increased proliferation rate compared to cADSCs. This might be due to abundant growth factors and nutrients in FBS.

Then, we reported that IACs displayed lower immunogenicity in an H3K27me3-HLA axis-dependent manner. Our group has previously found that ESC-derived MSCs significantly stimulate the proliferation of allogenic PBMCs during co-culture at day 3.<sup>4</sup> However, we did not observe the effects of ADSCs at this time point (the data are not shown). This phenomenon further indicates that ADSC



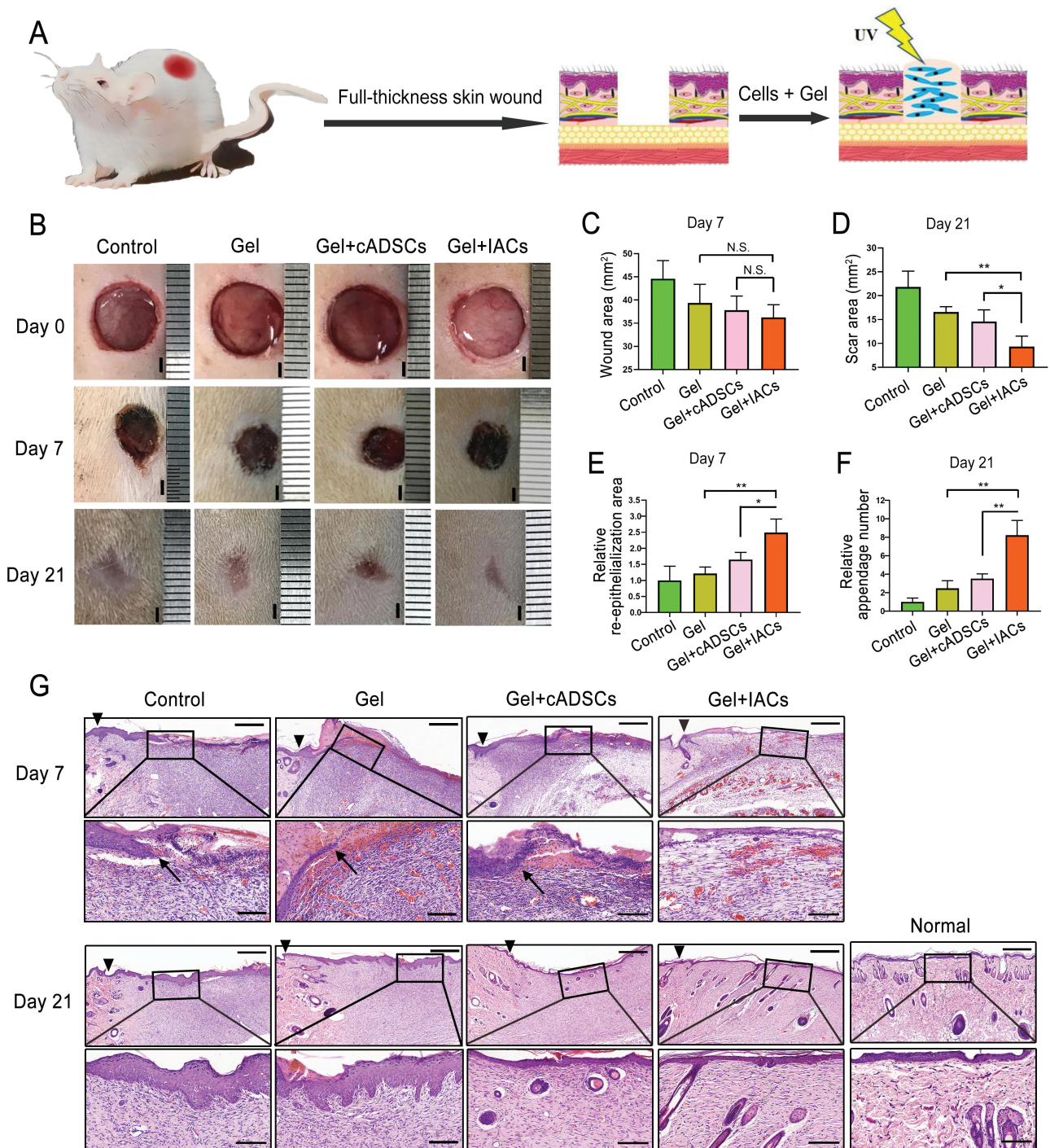


**Figure 6.** Xeno-transplantation of IACs with Gel further promotes skin repair. **(A)** A schematic protocol for skin repair by the cells incorporated in the Gel. **(B)** Gross view illustrating the skin regeneration in control, Gel, Gel + cADSCs, and Gel + IACs group at day 0, 7, and 21. Scale bar = 2 mm. **(C)** and **(D)** Quantified skin wound area at day 7 **(C)** and scar area at day 21 **(D)** for the 4 groups ( $n = 4$ ). **(E)** and **(F)** Quantification of relative re-epithelialization area at day 7 **(E)** and relative appendage number at day 21 **(F)** according to histological HaE staining ( $n = 4$ ). **(G)** Histological evaluation of the repaired skin by HE staining. Low magnifications: scale bar = 500  $\mu\text{m}$ . High magnifications: scale bar = 125  $\mu\text{m}$ . Arrowheads indicate the border between normal and regenerated tissues. Arrows indicate the terminal point of re-epithelialization.  $*P < .05$ ,  $**P < .01$ .

is a low-immunogenic cell type among different MSCs. Nevertheless, previous studies still found that ADSCs stimulate the secretion of inflammatory factors by PBMCs, trigger the proliferation of T cells, and induce severe T-cell-mediated cytotoxicity during long-term co-culture.<sup>5,33</sup> Our study showed that IACs significantly mitigated the immune cytotoxicity mediated by allogeneic PBMCs, which serves as

a novel candidate for low-immunogenic MSC. As for the further mechanism, H3K27me3 can inhibit the transcription of HLA-ABC in a conserved way in many types of cells, while the inhibitory effect in conventional MSCs is predicted to be weak.<sup>27</sup> Compared with cADSCs, our study found that the higher H3K27me3 protein expression level in IACs helped lowering HLA-ABC expression, thereby providing a new



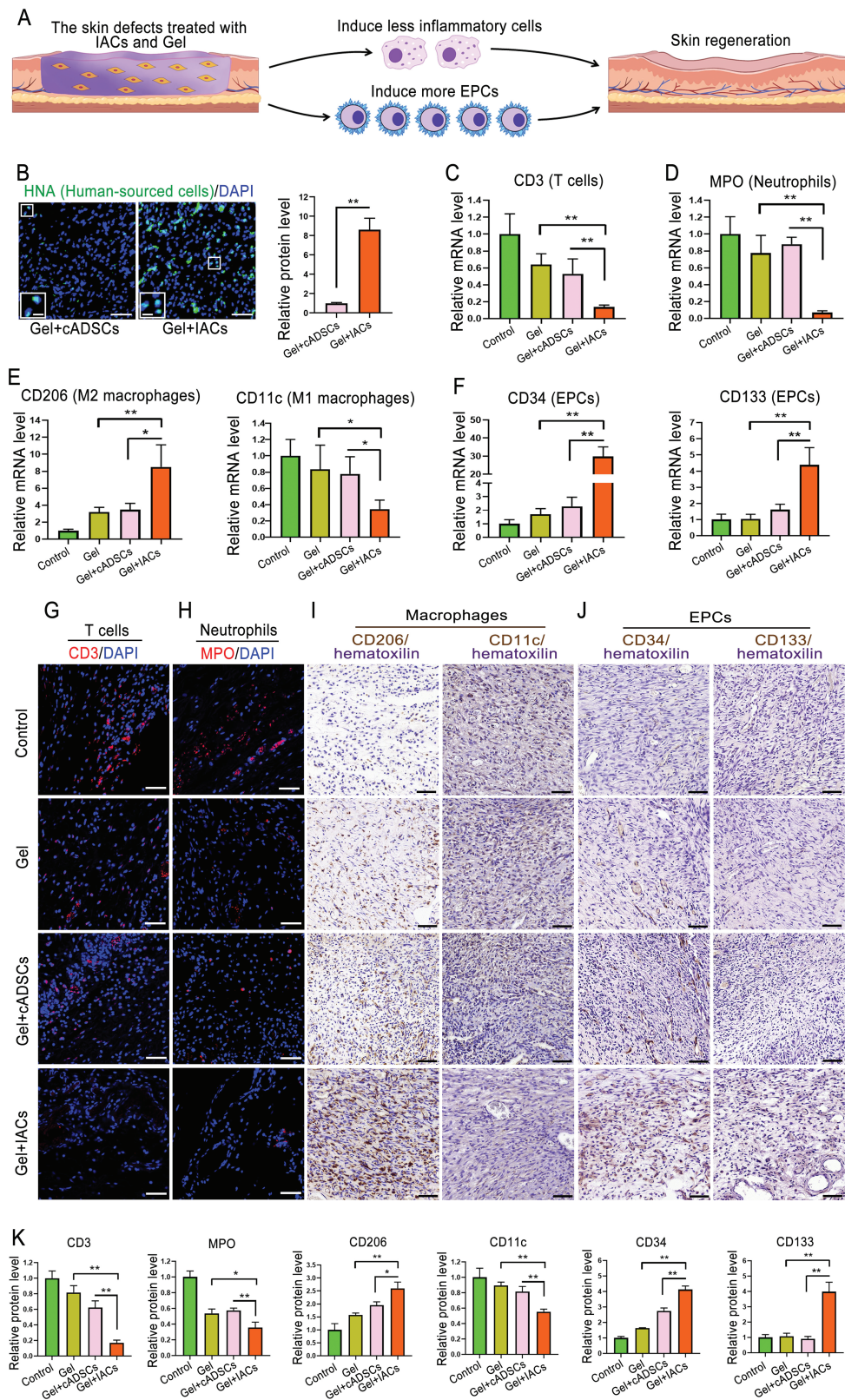


**Figure 7.** The immune microenvironment and angiogenic microenvironment of wound area at day 7. **(A)** A schematic illustration of the content of Fig. 8. **(B)** IF staining of human nuclear antigen (HNA) ( $n = 4$ ). Scale bar = 50  $\mu\text{m}$ . Inner scale bar = 12  $\mu\text{m}$ . **(C–F)** RT-qPCR analyzing the markers of CD3 (C), MPO (D), CD206 (E), CD11c (E), CD34 (F) and CD133 (F) at mRNA levels for control, Gel, Gel+cADSCs and Gel + IACs group ( $n = 4$ ). **(G and H)** IF staining of CD3 (G) and MPO (H) for the 4 groups. Scale bar = 50  $\mu\text{m}$ . **(I and J)** Immunohistochemistry staining of CD206 (I), CD11c (I), CD34 (J), and CD133 (J) for the 4 groups. Scale bar = 50  $\mu\text{m}$ . **(K)** Quantification of protein levels of CD3, MPO, CD206, CD11c, CD133, and CD34 ( $n = 3$ ). \* $P < .05$ , \*\* $P < .01$ .

potential target to modulate the immunogenicity of MSCs. It is also noteworthy that, compared with the cADSC group, although the immune response of PBMC in IACs + H3K27me3i group is slightly lower, the expression level of HLA-ABC in this group is higher, indicating that other factors also play a role in the immunogenicity of the cells. We speculate that the relatively high immunogenicity of cADSCs may also be correlated with, at least in part, xenogeneic proteins in FBS.<sup>34</sup>

Furthermore, we also demonstrated that IACs display stronger pro-angiogenic ability. Previous studies have documented the empowerment of the pro-angiogenic ability of conventional MSCs and MSC-derived exosomes by genetic modification and pretreatment of drugs, respectively.<sup>35,36</sup> In our study, we successfully enhanced the pro-angiogenic ability of ADSCs by utilizing a chemically defined culture. Yan et al. overexpressed N-cadherin in ADSCs (ADSC-Ncad) by adenovirus transduction and found that the ADSC-Ncad further promoted the tube formation of HUVECs by elevated secretion of HGF, MMP-13, and MMP-10 compared with cADSCs,<sup>9</sup> which is similar to the phenomenon that could be observed in IACs. Moreover, Yan et al also reported that  $\beta$ -catenin, a key protein in the Akt signaling pathway,<sup>37</sup> is responsible for the upregulation of the abovementioned pro-angiogenic factors.<sup>9</sup> Other studies also elucidated the role of the Akt signaling pathway in mediating the pro-angiogenic ability of MSCs.<sup>35,36</sup> We, therefore, considered that, despite using different methods, these studies and ours are proposing a similar mechanism, which is that the Akt signaling pathway plays a pivotal role in the pro-angiogenic ability of MSCs. As for the effects of the CM on HUVECs, a previous study reported that ADSCs modified with P-selectin binding peptide can increase the *e*NOS expression and NO production while inhibiting the expressions of the apoptosis-related genes in aHUVECs compared with the group without the ADSC treatment,<sup>8</sup> which is similar with the phenomenon observed in cADSCs in our study. Interestingly, IACs displayed stronger effects on these indices compared with cADSCs.

Finally, we have pilot-verified the enhanced regenerative functions of IACs in a full-thickness skin defect model. By transducing HCMV protein using retrovirus, Soland et al found that inhibition of HLA-I increases the survival of human MSCs in liver tissues of fetal sheep.<sup>38</sup> Consistent with such findings, the chemical-empowered IACs in our research also exhibited a higher survival rate compared with cADSCs while demonstrating lower expression of HLA-ABC. In the cases of xenotransplantation and allotransplantation, MSCs serve both as an immunosuppressor and an immunogen.<sup>1</sup> Correspondingly, a microenvironment with milder immunorejection can be attributed to the enhanced immunomodulatory ability and/or the lower immunogenicity of the cells.<sup>3,4,39</sup> As cADSCs and IACs showed comparable immunosuppressive capability, the lower immunogenicity of IACs might enable it to restrain the immune response in vivo. By contrast, the relatively high immunogenicity of cADSCs potentially masked their immunomodulatory ability. On the other hand, cADSCs have been reported to promote angiogenesis of impaired skin. Our study showed that IACs further promoted the formation of a pro-angiogenic microenvironment in vivo compared with the cADSCs group. We consider that this is due to, at least in part, the pro-angiogenic ability of IACs through superior paracrine effect as what our in vitro experiments have demonstrated. Besides, prolonged IACs survival, which leads to larger cell number, would also

contribute to cell function in this group.<sup>3</sup> As milder immunomicroenvironment and stronger pro-angiogenic microenvironment have been widely considered as the optimum condition to promote wound repair, including re-epithelization and the formation of cutaneous appendage,<sup>10,11,40</sup> the favorable properties of IACs contribute synergistically in accelerating the regeneration process.

In addition to what was mentioned above, other limitations for this research included (1) in this study, we used a chemically defined cocktail containing 13 factors, further screening (adding or deleting factors) could be performed to generate MSCs with lower immunogenicity and/or higher angiogenic ability. (2) Although the roles and mechanisms of a single factor have been reported, the mechanisms of how cells cultured in such a cocktail display these enhanced functions still need further illustration. (3) Besides skin defects in a rat model, repairing other challengeable defect models by IACs according to their advantages could be further studied. (4) Further illustrating the safety profile of IACs would pave the way for clinical tests.

## Conclusion

In this study, we have generated chemical-empowered human ADSCs termed as IACs by using a chemically defined cocktail in the culture medium. IACs exhibit typical MSC properties, robust safety profile, and enhanced stemness capacity. Compared with widely used cADSCs, IACs not only induce a significantly milder allogenic PBMC-mediated inflammatory response in an H3K27me3-HLA axis dependent manner but also strongly promote the NO production, their anti-apoptosis ability, and tube formation of HUVECs through superior paracrine signaling. The lower immunogenicity and stronger pro-angiogenic ability enable Gel-embedded IACs to promote faster tissue regeneration superior to cADSCs in a xeno-skin defect model. Taken collectively, IACs can be a promising candidate for future clinical tissue engineering and cytotherapy treatments.

## Funding

This work was supported by the National Key R&D Program of China (2017YFA0104900), the National Science Foundation of China (nos. T2121004, 31830029, 31800792).

## Conflict of Interest

The authors declare no potential conflicts of interest.

## Author Contributions

J.Y.: conceptualization, methodology, investigation, formal analysis, writing – original draft, writing – review and editing; J.Z.: conceptualization, methodology, investigation, formal analysis, writing – original draft; Q.Z.: conceptualization, investigation, formal analysis; X.C., Q.L.: investigation, formal analysis; R.Q.: investigation, writing – review & editing; R.L., F.W., Y.W., Y.Z.: investigation; X.Z.: conceptualization, data curation. G.C.: writing – review & editing; W.Z.: resources, data curation. H.L.: conceptualization, methodology, writing – review & editing; J.C.: conceptualization, resources, data curation, supervision,

writing – review & editing; H.O.: conceptualization, supervision, funding acquisition, project administration, writing – review and editing.

## Data Availability

All data needed to evaluate the conclusions in the paper are present in the paper and/or the Supplementary Materials. Additional data related to this paper may be requested from the authors.

## Supplementary Material

Supplementary material is available at *Stem Cells Translational Medicine* online.

## Reference

- Ankrum JA, Ong JF, Karp JM. Mesenchymal stem cells: immune evasive, not immune privileged. *Nat Biotechnol.* 2014;32(3):252-260. <https://doi.org/10.1038/nbt.2816>.
- Trounson A, McDonald C. Stem cell therapies in clinical trials: progress and challenges. *Cell Stem Cell.* 2015;17(1):11-22. <https://doi.org/10.1016/j.stem.2015.06.007>.
- Wu J, Song D, Li Z, et al. Immunity-and-matrix-regulatory cells derived from human embryonic stem cells safely and effectively treat mouse lung injury and fibrosis. *Cell Res.* 2020;30(9):794-809. <https://doi.org/10.1038/s41422-020-0354-1>.
- Wang Y, Huang J, Gong L, et al. The plasticity of mesenchymal stem cells in regulating surface HLA-I. *iScience.* 2019;15:66-78. <https://doi.org/10.1016/j.isci.2019.04.011>.
- Chang SH, Kim HJ, Park CG. Allogeneic ADSCs induce the production of alloreactive memory-CD8 T cells through HLA-ABC antigens. *Cells.* 2020;9(5):1246. <https://doi.org/10.3390/cells9051246>.
- Campeau PM, Rafei M, Francois M, et al. Mesenchymal stromal cells engineered to express erythropoietin induce anti-erythropoietin antibodies and anemia in allorecipients. *Mol Ther.* 2009;17(2):369-372. <https://doi.org/10.1038/mt.2008.270>.
- Zangi L, Margalit R, Reich-Zeliger S, et al. Direct imaging of immune rejection and memory induction by allogeneic mesenchymal stromal cells. *Stem Cells.* 2009;27(11):2865-2874. <https://doi.org/10.1002/stem.217>.
- Yan H, Mi X, Midgley AC, et al. Targeted repair of vascular injury by adipose-derived stem cells modified with P-selectin binding peptide. *Adv Sci (Weinb)* 2020;7(11):1903516. <https://doi.org/10.1002/advs.201903516>.
- Yan W, Lin C, Guo Y, et al. N-cadherin overexpression mobilizes the protective effects of mesenchymal stromal cells against ischemic heart injury through a beta-catenin-dependent manner. *Circ Res.* 2020;126(7):857-874. <https://doi.org/10.1161/CIRCRESAHA.119.315806>.
- An Y, Liu WJ, Xue P, et al. Autophagy promotes MSC-mediated vascularization in cutaneous wound healing via regulation of VEGF secretion. *Cell Death Dis.* 2018;9(2):58. <https://doi.org/10.1038/s41419-017-0082-8>.
- Zhou F, Hong Y, Liang R, et al. Rapid printing of bio-inspired 3D tissue constructs for skin regeneration. *Biomaterials.* 2020;258:120287. <https://doi.org/10.1016/j.biomaterials.2020.120287>.
- Zhao S, Li L, Wang H, et al. Wound dressings composed of copper-doped borate bioactive glass microfibers stimulate angiogenesis and heal full-thickness skin defects in a rodent model. *Biomaterials.* 2015;53:379-391. <https://doi.org/10.1016/j.biomaterials.2015.02.112>.
- Zhou W, Lin J, Zhao K, et al. Single-cell profiles and clinically useful properties of human mesenchymal stem cells of adipose and bone marrow origin. *Am J Sports Med.* 2019;47(7):1722-1733. <https://doi.org/10.1177/0363546519848678>.
- Brennan MA, Renaud A, Guilloton F, et al. Inferior in vivo osteogenesis and superior angiogenesis of human adipose-derived stem cells compared with bone marrow-derived stem cells cultured in xeno-free conditions. *Stem Cells Transl Med.* 2017;6(12):2160-2172. <https://doi.org/10.1002/sctm.17-0133>.
- Hong Y, Zhou F, Hua Y, et al. A strongly adhesive hemostatic hydrogel for the repair of arterial and heart bleeds. *Nat Commun.* 2019;10(1):2060. <https://doi.org/10.1038/s41467-019-10004-7>.
- Coutu DL, Francois M, Galipeau J. Inhibition of cellular senescence by developmentally regulated FGF receptors in mesenchymal stem cells. *Blood.* 2011;117(25):6801-6812. <https://doi.org/10.1182/blood-2010-12-321539>.
- Hur YH, Feng S, Wilson KF, et al. Embryonic stem cell-derived extracellular vesicles maintain ESC stemness by activating FAK. *Dev Cell.* 2020;56(3):277-277-291.e6.
- Beyaz S, Mana MD, Roper J, et al. High-fat diet enhances stemness and tumorigenicity of intestinal progenitors. *Nature* 2016;531(7592):53-58. <https://doi.org/10.1038/nature17173>.
- Zuo X, Xu W, Xu M, et al. Metastasis regulation by PPAR $\delta$  expression in cancer cells. *JCI Insight.* 2017;2(1):e91419. <https://doi.org/10.1172/jci.insight.91419>.
- Qin J, Yuan F, Peng Z, et al. Periostin enhances adipose-derived stem cell adhesion, migration, and therapeutic efficiency in Apo E deficient mice with hind limb ischemia. *Stem Cell Res Ther.* 2015;6(1):138. <https://doi.org/10.1186/s13287-015-0126-x>.
- Tontonoz P, Spiegelman BM. Fat and beyond: the diverse biology of PPAR $\gamma$ . *Annu Rev Biochem.* 2008;77(1):289-312. <https://doi.org/10.1146/annurev.biochem.77.061307.091829>.
- Li X, Guo W, Zha K, et al. Enrichment of CD146(+) adipose-derived stem cells in combination with articular cartilage extracellular matrix scaffold promotes cartilage regeneration. *Theranostics* 2019;9(17):5105-5121. <https://doi.org/10.7150/thno.33904>.
- Su R, Dong L, Li Y, et al. Targeting FTO suppresses cancer stem cell maintenance and immune evasion. *Cancer Cell.* 2020;38(1):79-96.e11. <https://doi.org/10.1016/j.ccell.2020.04.017>.
- Huang XP, Sun Z, Miyagi Y, et al. Differentiation of allogeneic mesenchymal stem cells induces immunogenicity and limits their long-term benefits for myocardial repair. *Circulation.* 2010;122(23):2419-2429. <https://doi.org/10.1161/CIRCULATIONAHA.110.955971>.
- Liu CT, Yang YJ, Yin F, et al. The immunobiological development of human bone marrow mesenchymal stem cells in the course of neuronal differentiation. *Cell Immunol.* 2006;244(1):19-32. <https://doi.org/10.1016/j.cellimm.2007.02.003>.
- Paczulla AM, Rothfelder K, Raffel S, et al. Absence of NKG2D ligands defines leukaemia stem cells and mediates their immune evasion. *Nature.* 2019;572(7768):254-259. <https://doi.org/10.1038/s41586-019-1410-1>.
- Burr ML, Sparbier CE, Chan KL, et al. An evolutionarily conserved function of polycomb silences the MHC class I antigen presentation pathway and enables immune evasion in cancer. *Cancer Cell.* 2019;36(4):385-401.e8. <https://doi.org/10.1016/j.ccell.2019.08.008>.
- Wedenoja S, Yoshihara M, Teder H, et al. Fetal HLA-G mediated immune tolerance and interferon response in preeclampsia. *EBioMedicine.* 2020;59:102872. <https://doi.org/10.1016/j.ebiom.2020.102872>.
- Gnani D, Romito I, Artuso S, et al. Focal adhesion kinase depletion reduces human hepatocellular carcinoma growth by repressing enhancer of zeste homolog 2. *Cell Death Differ.* 2017;24(5):889-902. <https://doi.org/10.1038/cdd.2017.34>.
- Yang MH, Zhao L, Wang L, et al. Nuclear lncRNA HOXD-AS1 suppresses colorectal carcinoma growth and metastasis via inhibiting HOXD3-induced integrin beta3 transcriptional activating and MAPK/AKT signalling. *Mol Cancer.* 2019;18(1):31. <https://doi.org/10.1186/s12943-019-0955-9>.
- Garcia V, Parka EJ, Siragusa M, et al. Unbiased proteomics identifies plasminogen activator inhibitor-1 as a negative regulator of endothelial nitric oxide synthase. *Proc Natl Acad Sci USA.* 2020;117(17):9497-9507.



32. Zhang Y, Lei T, Tang C, et al. 3D printing of chemical-empowered tendon stem/progenitor cells for functional tissue repair. *Biomaterials*. 2021;271:120722. <https://doi.org/10.1016/j.biomaterials.2021.120722>.
33. Chang SH, Park CG. Allogeneic ADSCs induce CD8 T cell-mediated cytotoxicity and faster cell death after exposure to xenogeneic serum or proinflammatory cytokines. *Exp Mol Med*. 2019;51(3):1-10. <https://doi.org/10.1038/s12276-019-0231-5>.
34. Jung S, Panchalingam KM, Rosenberg L, et al. Ex vivo expansion of human mesenchymal stem cells in defined serum-free media. *Stem Cells Int*. 2012;2012:123030. <https://doi.org/10.1155/2012/123030>.
35. Yu M, Liu W, Li J, et al. Exosomes derived from atorvastatin-pretreated MSC accelerate diabetic wound repair by enhancing angiogenesis via AKT/eNOS pathway. *Stem Cell Res Ther*. 2020;11(1):350. <https://doi.org/10.1186/s13287-020-01824-2>.
36. Liang X, Ding Y, Lin F, et al. Overexpression of ERBB4 rejuvenates aged mesenchymal stem cells and enhances angiogenesis via PI3K/AKT and MAPK/ERK pathways. *FASEB J*. 2019;33(3):4559-4570. <https://doi.org/10.1096/fj.201801690R>.
37. Zhang J, Shemezis JR, McQuinn ER, et al. AKT activation by N-cadherin regulates beta-catenin signaling and neuronal differentiation during cortical development. *Neural Dev*. 2013;8(1):7. <https://doi.org/10.1186/1749-8104-8-7>.
38. Soland MA, Bego MG, Colletti E, et al. Modulation of human mesenchymal stem cell immunogenicity through forced expression of human cytomegalovirus us proteins. *PLoS One*. 2012;7(5):e36163. <https://doi.org/10.1371/journal.pone.0036163>.
39. Yoshida K, Nakashima A, Doi S, et al. Serum-free medium enhances the immunosuppressive and antifibrotic abilities of mesenchymal stem cells utilized in experimental renal fibrosis. *Stem Cells Transl Med*. 2018;7(12):893-905. <https://doi.org/10.1002/sctm.17-0284>.
40. Eming SA, Martin P, Tomic-Canic M. Wound repair and regeneration: mechanisms, signaling, and translation. *Sci Transl Med*. 2014;6(265):265sr-26266.